Pedological stratification effect of corrosion and contamination products on Byzantine bronze artefacts

I. Sandu*[1], N. Ursulescu[2], I. G. Sandu[3], O. Bounegru[2], I. C. A. Sandu[4] and A. Alexandru[5]

The present paper deals with the identification of six ancient Byzantine bronze coins found in the same archaeological site of Nufarul (Tulcea County, Romania), by corrosion product and alloy analysis. The microstratigraphies (i.e. layers), together with microchemical tests including reflection colorimetry, IR spectroscopy, X-ray diffraction and scanning electron microscopy assisted by X-ray spectrometry have rendered evident the stratified morphology of three types of patina. They are the primary type resulting from redox processes, the secondary type determined by acid–base and related hydrolytic processes and the ternary type (or the contamination patina) from segregation, diffusion and osmosis processes. The stratigraphical distribution of the chemical components in the structure of the patina is caused by the pedological (soil) processes at the archaeological sites and can be the main factor used in the authentication of ancient bronze artefacts.

Keywords: Bronze coins, Archaeological patina, Microchemical tests, Microstratigraphy, FTIR spectroscopy, SEM-EDX analysis, Reflection colorimetry, Pedological transformation

Introduction

Metals, as compared to other materials, have a unique behaviour that often results in the creation of artefacts in archeological investigation. These include, for noble metals, a high resistance to external environmental factors, and for base metals, a return to the mineral state through the processes of corrosion and erosion.[1–3] Among key Cultural Heritage assets, coins and other metallic numismatic pieces offer many examples of the conservators' art and, in the research field, they can be good samples to be used for experiments. However, except for treasure trove hoards, coins are not always easily discovered by excavation if dispersed in archaeological sites.[2]

Excepting the treasure hoards that consist of noble metals, the finds made of other metals have the disadvantage of a precarious conservation state. The two worst cases are precollapse where they are preserved as pieces with a very thin metallic bulk that merely preserves their shape, or collapse where the metallic bulk is completely absent and the shape cannot be recognised. In such cases their authentication is almost impossible.[1–5] Among these cases, pieces made of ancient bronze have a very complex composition of corrosion products, resulted from the reactions with the environment (i.e. chemical, electrochemical or microbiological), or by contamination, during the various soil based (pedological) processes (i.e. segregation, cementation, monolithisation, recrystallisation, etc.). The most important problems arise for those pieces that do not contain any residual metallic bulk. Such pieces are often destined to the 'grey fund' and abandoned in most cases during the preliminary classification immediately after excavation. These pieces can be a very important source of information, mainly about the basic mineral and often being the unique proofs of a technique or metallurgical tradition/period.

The present paper studies the comparative chemical and mineralogical distribution for six bronze coins of the Byzantine period, some of which retain the metallic bulk and some are entirely corrosion products. Modern methods of microstratigraphical analysis are used in the present work, including microchemical tests, reflection colorimetry, Infrared (IR) spectroscopy, X-ray diffraction (XRD) and scanning electron microscopy with X-ray spectrometry (SEM/EDX). These allow the determination of the archaeological/geological characteristics (mineral and alloy composition) used for the authentication of the coins, and in establishing the basic mineral, the manufacturing period and the original area of production. The purpose is to identify the elements

[1]Department of Cultural Heritage, University of Iasi, 9 Closca St., 700066 Iasi, Romania
[2]Department of Archaeology, University of Iasi, 11 Carol I Blvd., 700506 Iasi, Romania
[3]Department of Teachers Training, Technical University of Iasi, 71 D. Mangeron Blvd., 700050 Iasi, Romania
[4]Romanian Inventors Forum, 3 Sf. Petru Movila St., 700089 Iasi, Romania
[5]Faculty of Materials Science and Engineering, Technical University of Iasi, 71 D. Mangeron Blvd., 700050 Iasi, Romania

*Corresponding author, email ion.sandu@mail.dntis.ro

Published by Maney on behalf of the Institute
Received 2 February 2007; accepted 24 June 2007
DOI 10.1179/174327807X234688

coming from the alloy (obtained from the mineral) and the contamination that arises from the interactions with the environment.

Introduction and basis of study

According to the previous studies,[1–5] for ancient bronze coins, including those with and without remaining bulk metal and coming or not from disturbed sites, three types of surface deposits can be differentiated in the structure of the archaeological patina. The first type is the result of redox processes, the second acid–base, complexation and hydric processes (i.e. mainly through hydrolysis and ionic exchange) and the third is those resulting from processes of site contamination (diffusion, segregation, deposition, etc.). These deposits/products are formed at different stages, and are characteristic of specific types of patina. Thus, oxides and sulphides, formed since the utilisation period, constitute the primary patina. Halogenides, oxyhydroxides, carbonates, sulphates, phosphates, etc., which formed in the final period of utilisation (i.e. before abandonment) and in the first step of the pedological period, define the secondary patina. Finally, those resulting from the physical processes of diffusion–segregation–deposition–recrystallisation constitute the contamination patina.[3]

The study of these products allows not only an explanation of the mechanisms of the formation but also the determination of chronological parameters, which can identify factors useful for the authentication of the find. These include the nature of the alloy and its mineralisation, the method of manufacture, the provenance of the coin (i.e. period and place of creation), the method and period of utilisation, as well as other data concerning the 'time imprint'.[6–8] Thus, the stratigraphical depth of the site in time, from the surface where climatic, microbiological and anthropological agents are strong and cyclic, towards the internal zones where aerobic or anaerobic conditions may vary as a function of oxygen and water constant in the soil. These have oscillations in time that create different systems of cyclic variation all of which play important roles in identifying the corrosion products, and the chemical (e.g. ionic exchange) and contamination events that occur over burial time. However, the last cyclic processes occur at a very low rate during the centuries and produce the important structural modification of the ancient patina of an object, creating a stratigraphical distribution of the three groups of products. The cyclic properties of the pedological processes determine the specific stratification of the three types of patina, which can be rendered evident by an analytical study.

For example, Fig. 1 compares the microstratigraphies of the archeological patinas on two coins coming from different sites. One site (Fig. 1*a*) was without disturbance and with a low, almost constant humidity, and the other (Fig. 1*b*) was situated in an area with a great mobility of subterranean water and a complex chemistry. The stratigraphical distribution, in the form of deposits of products specific to the three types of patina, i.e. primary, secondary and of contamination, can be seen for the first coin[6] with a different deposition of microcrystals that are not uniform in the volume phase of the archaeological patina for the second coin.[3] If in the case of a non-disturbed site, the structural and

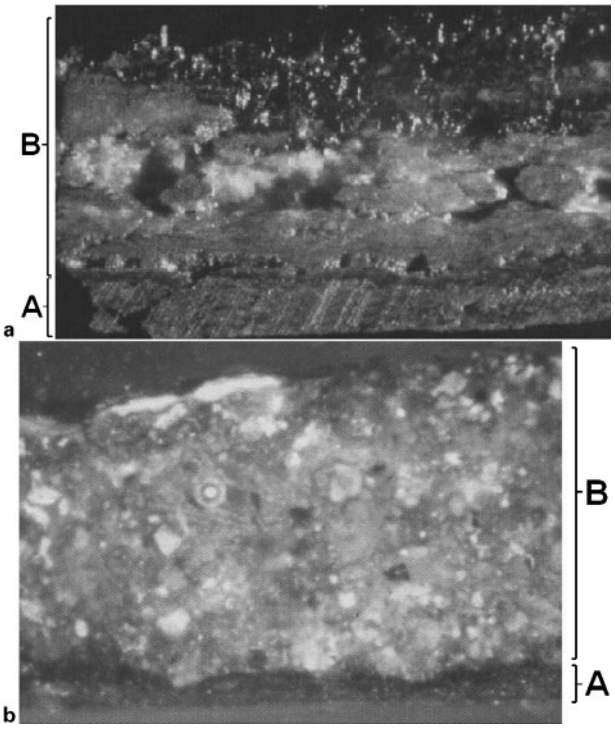

a patina for coin coming from archaeological non-disturbed site and with low humidity;[6] *b* patina for coin coming from archaeological site with fluctuant chemistry produced by abundant subterranean water[3]

1 Microstratigraphical structure of archaeological patina: A – metal support, B – corrosion layer (×100)

phenomenological correlations for the chronological valuations can be deduced, for the second one, the study of the parameters implied in such correlations requires either complex analyses or the corroboration of new methods and techniques of higher resolution.

In summary, the stratigraphical morphology of most archaeological patinas of ancient bronze pieces has a sandwich structure, characteristic of the Liesegang effect,[6] in which the layers of the primary patina are overlapped or partially interposed with the ones of the secondary patina. The layers of contamination products, formed during the chemical chronological processes that occur in the heterogeneous liquid–solid systems, with a sequential formation of products with a characteristic morphology, are also named 'Liesegang rings'. In the case of bronze coins, the primary patina generally contains layers of cuprite or cuprite/tenorite (i.e. copper oxides) and copper sulphides. The secondary patina contains malachite/azurite (i.e. copper hydroxy carbonates), overlapped or alternated with layers of athacamite/parathacamite (i.e. copper hydroxyl chlorides) and brochantite/anthlerite (i.e. copper hydroxy sulphates) and of contamination products such as the ankerite (calcium–magnesium carbonates), gypsum (calcium sulphate), silicates, clays and other metallic mineralisation (e.g. by cassiterite – SnO), resulting from the segregation and diffusion processes in the inferior layers.[3,9–12]

Experimental techniques

A group of ancient bronze coins, discovered in 2000,[13] on the territory of Romania, from the Nufarul archaeological site (Tulcea County), have been studied. Six

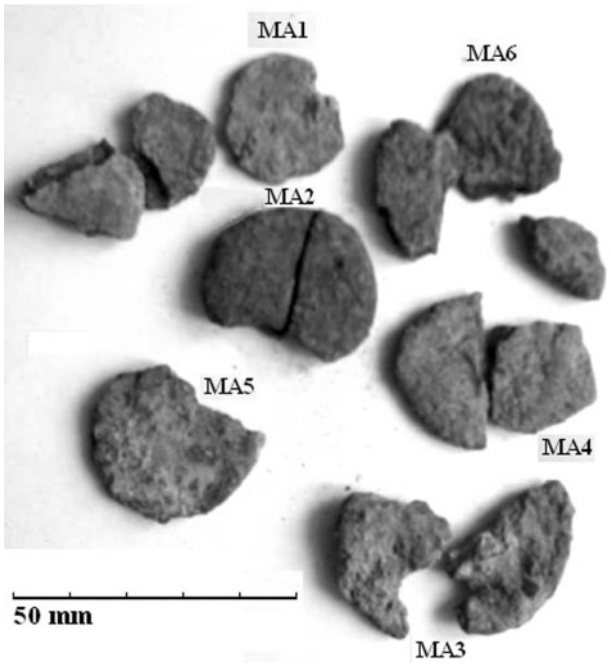

2 Bronze coins from Nufarul treasure, from where six coins were selected for analyses

coins were found separately in the site, over an area of ~ 600 m^2. To analyse the corrosion products and the surface contaminants, the following techniques were applied: microphotography on normal cleaned samples, with or without standard metallographic etching, and on stratigraphical sections (transversal sections), microchemical analysis, reflection colorimetry, IR spectroscopy, XRD and analytical SEM (e.g. by EDX).

Coins taken into study

The present study has been carried out on six ancient coins from the eleventh and twelfth centuries, which are designated here as MA1, MA2, MA3, MA4, MA5 and MA6. They are shown in Fig. 2. All these coins were initially classified for the 'grey fund' (i.e. not examined further); some of them conserve a fragile metallic bulk, however, others do not.

Microchemical and stratigraphical analysis

Both the transversal sections and the surfaces of the coins have been analysed by optical microscopy using an OLYMPUS CX21 microscope under reflected light (Vis), followed by microchemical tests. The micrographs were taken using an OLYMPUS digital camera, adapted to the microscope. The nature of the corrosion products and the contaminants was established by the microchemical reactions on the surfaces or the transversal sections, in their native state or after the previous mechanical or chemical cleaning. The nature of the structural components of the corrosion products and contaminants, disposed in concentrated areas as attractively coloured crystals, has been directly attributed, based on their colour and crystallographic system.[14]

Reflection colorimetry

The colorimetric study has been performed by selecting the areas with corrosion products and the area with a uniform patina on the surface of the coins. An optical fibre digital colorimeter with different illumination geometries and observation angles has been connected to a computer with which the values of red–green–blue (RGB) hues and intensities in the CIE colorimetric triangle have been established. The analysed areas were masked off to provide small holes delimiting the measuring areas. The number of 3–5 points corresponds to the comparison areas (basic alloy and patina). In each point the transducer has been positioned directly on the material to obtain the colour directly from the surface.[15]

X-ray diffraction

X-ray diffraction analysis was carried out on finely grinded powders of crystallites. A Philips 1130/00 diffractometer, equipped with a Cu anode and a Ni filter (for high resolution), at 1200 W and vertical goniometer with an angular resolution $>0{\cdot}005^\circ$ has been used for this purpose.[16,17]

Infrared spectroscopy

Infrared analysis was performed on powder samples dispersed in KBr pellets. The IR spectra were taken from 200–4000 wavenumbers (cm^{-1}), using a Carl Zeiss Jena SPECORD M80 spectrophotometer.[18]

Scanning electron microscopy and X-ray spectrometry

Scanning electron microscopy was carried out using a HITACHI S2600N electron microscope with an EDX spectrometer, with two functions. The present study was carried out at an accelerating voltage of 15 kV, with typical analyses taken at magnifying powers of $\times 250$ to $\times 300$ and the distribution mapping of up to eight elements on surface of the six coins.[3]

Results and discussion

Table 1 shows the images and the shape of the Byzantine coins, together with the microstratigraphy on fractured and polished cross-sections, examined with the optical microscope at a magnifying power of $\times 40$. According to the purpose of the paper, the authors will identify the elements coming from the metal and those resulting from corrosion due to contamination.

Mineralogical composition of cross-section structure of Ancient bronze coins

Considering that old bronzes are composed mainly of four metals, namely Cu, Sn, Zn and Pb as well as small quantities of other elements such as Fe, Sb, Al, As, Si and P, the visual microscopy has allowed the study of the morphology of the microcrystallites on the surfaces and in the sections. Successive microchemical tests with specific reagents have contributed to the determination of the mineral components of the corrosion products and contaminants formed either over time or by pedological processes. It should be emphasised that the coins dated from the eleventh and twelfth centuries have a very thick corrosion layer, with an important quantity of organic and inorganic contaminants. The metallic bulk noticed in the stratigraphical section shows the segregation of Zn with its accumulation on the surface.

Microchemical qualitative analysis

During the formation of the archaeological patina, each metal of the ancient basic alloy (copper, zinc, tin, lead, iron, etc.) makes up specific products resulted from the pedological processes and the bronze coins are characterised by a great number of mineral species which are

given in Table 2. On the surface of the coins the chemistry of these products is quite well differentiated, depending not only on the exogenous agents related to the climatic environment, the site place and its aggressive character, etc., but also on the endogenous ones related to the alloy elaboration, the origin mineral and the metallurgical technology.

On analysing the data from Table 2, a similarity can be noticed between the concentration and the products from the archaeological patina for the MA1 and MA3 coins (containing Cu, Sn, Zn, Fe, Cr), the MA2 and MA4 (containing Cu, Sn, Pb, Zn), MA5 and the MA6 ones (containing Cu, Sn, Zn, Fe) respectively.

All non-metallic anions come from the chemical system of the archaeological site. Exceptions are the double and saline oxides (ZnO_2^{2-}, SnO_3^{2-}, CrO_3^{2-}, etc.) which probably derive from the alloys. From the first group, the majority of the oxide and sulphide anions are from the primary patina and the others from the secondary and tertiary patinas respectively. The

Table 1 State and aspect of coins and metallic bulks

	Image of the coins	Shape of the coins	Break/polished cross-section (×40)	State of the metallic bulk
MA1		Flat, convex	 	Thin, affected by corrosion after the removal from the site; advanced segregation process with holes and fissures between phases
MA2		Thick	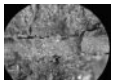 	Very thick, unaffected by corrosion after break; advanced segregation processes with holes and fissures between phases
MA3		Thin, very soil	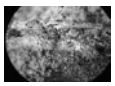 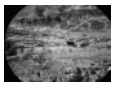	Thin, spongy, very affected by corrosion after site extraction, non-uniform small holes and shrinks
MA4	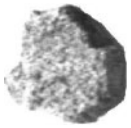	Thick	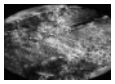 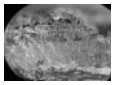	Thick, compact, unaffected by corrosion after site extraction, good stratification
MA5	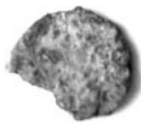	Thin	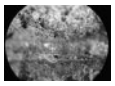 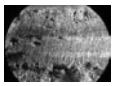	Thin, compact, affected by corrosion after break, good stratification
MA6		Thin, flat	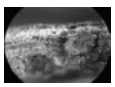 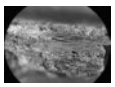	Very thin and corroded after break, good stratification

Table 2 Chemical compounds determined by mineralogical analysis in corrosion products and contaminants from surface of coins*

Mineral phase	Chemical formula	Colour and aspect	MA1	MA2	MA3	MA4	MA5	MA6
Cuprite	Cu_2O	Brick red with grey brownish or yellowish to orange tones	+++	+++	+++	++++	+++	+++
Tenorite	CuO	Black grey to brown	++	+	++	+	++	+
Malachite	$CuCO_3Cu(OH)_2$ or $Cu_2(OH)_2CO_3$	Green with a characteristic vitreous aspect	++++	+++	++++	+++	++++	+++
Azurite	$2CuCO_3Cu(OH)_2$ or $Cu_3(OH)_2(CO_3)_2$	Dark blue	++	++	++	++	++	++
Athacamite	$Cu_2(OH)_3Cl{\cdot}nH_2O$ or $CuCl_2{\cdot}3Cu(OH)_2{\cdot}2nH_2O$	Emerald green with more or less dark tones in function of vitreous aspect	++	+	++	+	++	++
Parathacamite	$Cu_2(OH)_3Cl$ or $CuCl_2{\cdot}3Cu(OH)_2$	Green blue	+	−	+	−	+	+
Nantokite	Cu_2Cl_2	Light grey with wax aspect	++	+	++	++	++	++
Chalcocite (Calcosine)	Cu_2S	Pb-like grey with metallic brightness	−	++	−	++++	++	+
Calconit e	$CuSO_4{\cdot}5H_2O$	Clear blue	−	+	−	+	++	++
Anthlerite	$Cu_3(OH)_4SO_4$ or $CuSO_4{\cdot}2Cu(OH)_2$	Blackish with green tones	−	+	−	+	++	++
Brochantite	$Cu_4(OH)_6SO_4$ or $CuSO_4{\cdot}3Cu(OH)_2$	Blue to clear green	−	+	−	+	++	++
Langite	$Cu_4(OH)_6SO_4{\cdot}H_2O$ or $CuSO_4{\cdot}3Cu(OH)_2{\cdot}H_2O$	Dark bright green	−	+	−	+	++	+
Cassiterite	SnO_2	Shine White	++	++	++	++	++	++
Tin sulphid	SnS	Black	−	++	−	++++	+	+
Minium	Pb_3O_4	Red	−	+	−	−	−	−
Anglesite	$PbSO_4$	Grey green	−	+	−	+	−	−
Cerrusite	$Pb_2(OH)_2CO_3$	White	+	+	+	+	+	+
Gloslarite	$ZnSO_4{\cdot}\ 7H_2O$	Grey opalescent	+	+	+	+	+	+
Goetite	FeO(OH)	Bright (nacre) white	+	−	+	−	+	+
Cromite	$FeCr_2O_4$	Dark blue	+	−	+	−	−	−
Calcite	$CaCO_3$	White grey	+	++	+	++	+	+
Gypsum	$CaSO_4{\cdot}2H_2O$	White grey	++	−	+	−	++	+
Clorapatite	$Ca_5Cl(PO_4)_3$	White grey	++	++	++	++	+	+
Hydroxoapatite	$Ca_5(OH)(PO_4)_3$	White grey	+	+++	+	+++	−	++
Ankerite	$Ca(Fe,Mg)(CO_3)_2$	Translucent	++	+++	++	+++	+	+
Quarz	SiO_2	Translucent grey	+++	++	+++	++	++	++
Caolinite	$Al_2[(OH)_4Si_2O_5]$	Translucent white grey	+	++	+	−	++	+

*-: absent; +: very rare; ++: rare; +++: small dispersed deposits; ++++: large dispersed deposits.

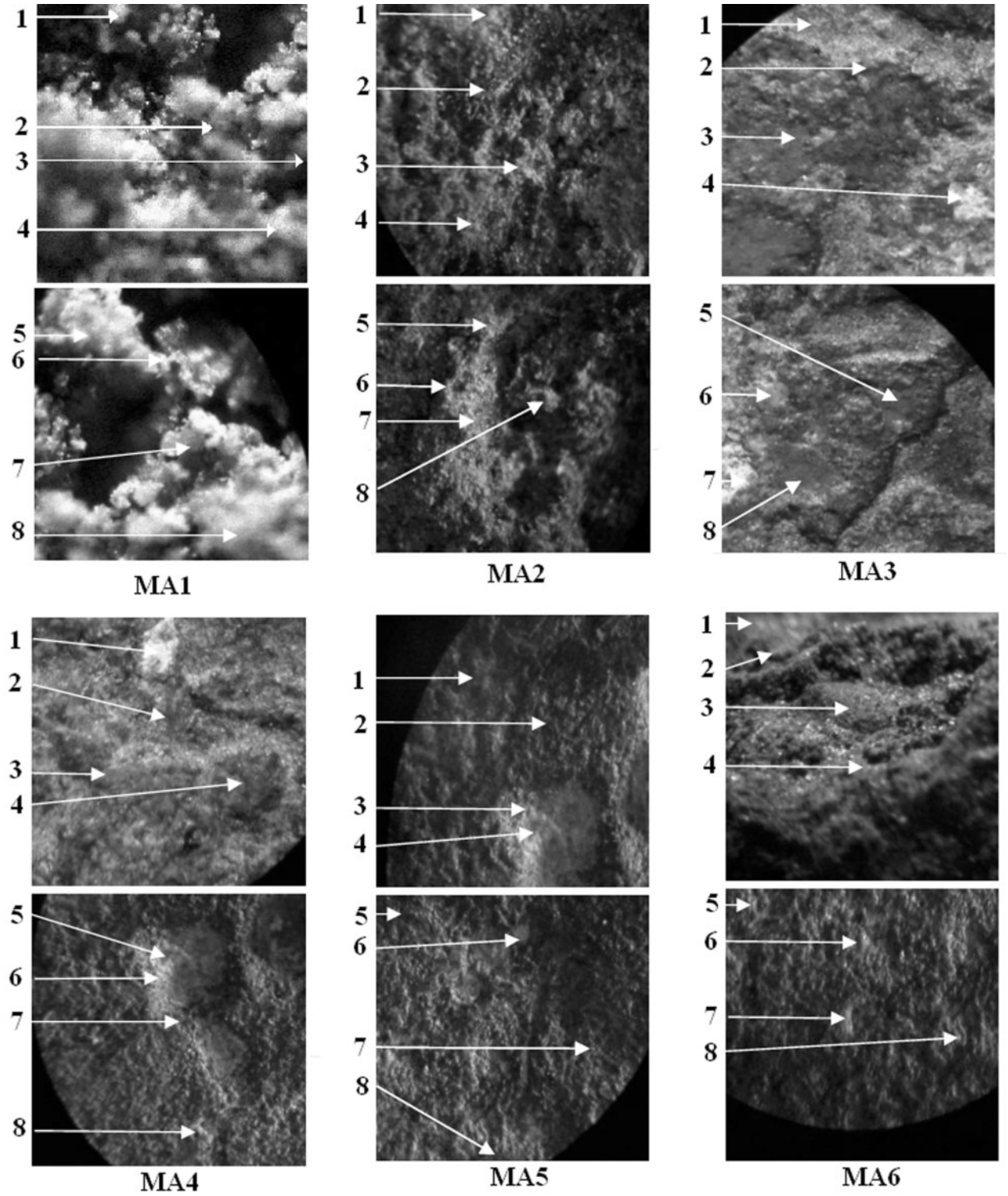

3 Sampling areas for colorimetric analysis (×240 for MA1 and ×40 for MA2 to MA6): points 1 to 4 are obverse of coins and points 5 to 8 are reverse side

compounds from the tertiary patina have contamination cations from the site, e.g. Ca(II), Mg(II), Al(III) and Si(IV).

Colorimetric analysis

Based on the microchemical analyses regarding the chemical nature of the corrosion products, which occur mainly as coloured minerals, the areas for the colorimetric analysis by reflection have been selected under an optical microscope (Fig. 3). The points selected for analysis are represented by the mineralogical entities from the surface of the coins, both during the corrosion processes and by the contamination after the pedological processes (recrystallisation dehydration, segregation, osmosis, carbonation, sulphation, chlorination, etc.). Colorimetry has an advantage that allows a rapid analysis of the microcrystallites. In this respect, the mineralogical phases, also studied with other methods, have been, for the major part, identified (Table 3). The measured deviations and the chromatic alterations can

be evaluated with the relative colour modifications of the morphologically similar microcrystallites from Table 3. The main purpose has been the correlation between the colorimetric data concerning the identification of the mineralogical phases.

The IR spectra (Table 4) and the X-ray diffractograms (Table 5) have identified the complex nature of the corrosion products in the three groups of coins. Twenty mineral compounds have been identified in the diffractograms for the three groups of coins, the main part of them being formed by corrosion, others by contamination, such as gypsum, quartz, calcite and a limited series of organic compounds. On analysing the data from Tables 4 and 5, a parallelism can be established between MA1 and MA3, MA2 and MA4, MA5 and MA6 coins respectively. For example, MA2 and MA4 have chemical species specific for the primary patina with a high concentration in sulphides. The complexity of the spectra and the diffraction patterns increases from MA1, MA3 to MA2, MA4 to MA5, MA6. This aspect is interpreted not only because of the alloy composition and the age of the artefact, but also as an effect of the aggressive action of the exogenous factors that modified the material. It is also true that some endogenous factors, related to the material and the creation technology, together with the exogenous ones, have determined in most cases the mechanism of the degradation and deterioration processes. Many ancient coins have been exposed to strong pedological processes (erosion and corrosion) or to thermal ones, processes that have made them fragile, thus producing phase modifications, irreversible in most cases.

SEM-EDX analysis

The SEM for the six studied coins has rendered evident on their surfaces a rough and non-homogeneous structure, with uneven relief and microfissures and mineral deposits resulting not only from deposition and monolithisation, but also from the segregation in the volume phase (Fig. 4).

For coins MA2 and MA4, many pores and microcrystals were observed that were non-uniformly distributed on the surface. On the same surface area from where the SEM photography has been taken, EDX microanalysis was also carried out, the results of which indicate the presence, together with copper, not only of some other alloy elements of mineral origin specific to the ancient bronze, such as Pb, but also of the anions resulted from the corrosion and the ionic exchange processes such as carbonates, sulphates and chlorides and the contamination products based on Si, Ca, K and Mg.

The main difference between the coins consists in the different distributions of the elements specific to the anions and the contamination products. A similarity should also be noticed between the contamination products for the MA1 and MA3 coins, the MA2 and MA4, the MA5 and MA6 ones respectively. On analysing the comparative distribution of elements in the surfaces, a clear distinction between species from the alloy and those resulting from the corrosion and ionic exchange as well as from contamination can be determined. The first ones have a relatively uniform distribution (Cu, Fe, Sn, Zn, Pb, etc.), however the others have a zonal concentration (Si, Ca, Al, S, etc.). The apparent uniformity in the distribution of K, Mg, Ca and Cl may be explained as an effect of the segregation, the ionic exchange and the insolubility in the form of double salts (ankerite, carnalite, hydroxiapatite, clorapatite, etc.).

The non-uniformity in the mineral distribution on the surface at the MA1, MA3, MA5 and MA6 coins can also be noticed, especially those arising from contamination processes and mineral concentrations. The MA2 and MA4 coins have a surface non-uniformity and a highly non-homogeneous distribution of the two products groups, namely of the contamination and of the corrosion/ionic change. The coins also have deep and big pores. The MA4 coin has on its distribution map a high concentration of sulphide ions from the primary patina. The MA1 and MA3 coins have very similar compositions and the presence of Cr and Fe cations, as alloy microelements, which are not present at all in the coins, demonstrates that these two coins are made from the same mineral.

Table 3 Colorimetric results (RGB) for minerals in structure of patina analysed by groups of coins

		MA1				MA2				MA3		
No. crt.*	Mineral	R	G	B	Mineral	R	G	B	Mineral	R	G	B
1	Cuprite	211	55	0	Paratachamite	159	136	30	Tenorite	180	100	5
2	Cuprite	215	82	15	Minium	220	125	41	Brocantite	78	84	10
3	Calcite	255	236	209	Tenorite	175	88	9	Cuprite	195	62	17
4	Quartz	216	157	39	Calcocite	125	114	22	Ceruza	249	255	157
5	Calcite	231	246	57	Tenorite	160	116	7	Cuprite	153	45	0
6	Malachite	75	140	14	Atacanite	149	152	19	Atacanite	139	164	36
7	Malachite	58	117	51	Malachite	84	108	24	Gypsum	241	252	124
8	Calcite	251	241	109	Paratachamite	134	135	31	Cuprite	182	56	16
		MA4				MA5				MA6		
1	Quartz	234	244	122	Brocantite	63	61	13	Antlerite	100	76	6
2	Cuprite	138	58	9	Tenorite	184	80	9	Langite	159	147	27
3	Malachite	62	125	21	Atacanite	135	130	10	Calcocite	165	118	28
4	Cuprite	140	49	5	Cassiterite	236	212	62	Cuprite	158	75	7
5	Anglesite	104	85	0	Nantokite	63	31	8	Antlerite	106	36	0
6	Gloslarite	242	206	84	Anglesite	112	99	7	Brocantite	57	55	6
7	Tenorite	211	109	24	Cuprite	192	100	35	Cuprite	170	95	2
8	Calcite	219	183	63	Cuprite	180	83	41	Cassiterite	231	157	60

*Points 1 to 4 are the obverse of coins and points 5 to 8 are the reverse side.

Thus, in general it can be said that the data from the SEM-EDX analysis are very well correlated with those of the microchemical, IR, X-ray and colorimetric analysis, all of which assists in determining the pedological and original history of the buried artefact.

Concluding remarks

For ancient bronze coins and other metallic pieces discovered in archaeological sites, a detailed analysis can render evident a series of structural elements specific to the archaeological patina that allows the differentiations in the mineral and alloy, the area where the artefact was made and the location and period of utilisation to be determined. In the case of the recovered samples without metallic bulk that are very difficult to identify, it is very important to establish which elements in the alloy (including the microelements) are from the mineral, and which arise from the contamination of the site or from the environment.

During the interment of the sample in the site, soil based (pedological) processes cause continuous physical and chemical transformations to the surface of the pieces, the contamination patina being overlapped on the primary and secondary ones. When the processes are on the surface, under the influence of the climatic agents, the ancient metal patina conserves the shape of the object quite well, but once the stratigraphical layering begins, the pedological cyclic processes lead to the segregation of the compounds into different layers resulted from the three types of reactions described above. Depending on the mechanical fluctuations of the

Table 4 Characteristic group vibrations for main chemical species

Coin	Mineral	Dominant species	Characteristics group vibrations, cm^{-1}
MA1	Cuprite	Cu_2O	330s, 400p
	Zincite	$ZnCO_3$	460p
	Tenorite	CuO	500p
	Calconite	$CuSO_4{\cdot}5H_2O$	610m
	Cromit/Cromat/Aluminat	$Cr_2O_4^{2-}/CrO_4^{2-}/AlO_2^-$	790m, 800s
	Atacamite/paratacamite	SO_4^{2-}	1050f
	Quarz	SiO_2	1100p
	Malachite	CO_3^{2-}	1400p, 1500p
	Gypsum	$CaSO_4{\cdot}2H_2O$	1610p
	Malachite	HO^-	3370p, 3450p
MA2	Sulphide/tin oxide	S^{2-}/SnO_3^{2-}	300 – 330p
	Zincite/quarz	$ZnCO_3/SiO_2$	480m
	Tenorite/aluminate	CuO/AlO_2^-	520s, 610m
	Malachite/calcite	CO_3^{2-}	630m, 900s
	Atacamite/paratacamite quarz	SO_4^{2-}	1055p
	Malachite	SiO_2	1080p
	Malachite	CO_3^{2-}	1400p, 1500p, 1640p
		HO^-	3350p, 3440p
MA3	Cuprite	Cu_2O	330s, 400p
	Zincite	$ZnCO_3$	450p
	Tenorite	CuO	500p
	Calconite	$CuSO_4{\cdot}5H_2O$	610p
	Cromit/Cromat/Aluminat	$Cr_2O_4^{2-}/CrO_4^{2-}/AlO_2^-$	630p, 850m
	Atacamite/paratacamite	SO_4^{2-}	1000p, 1050p
	Quarz	SiO_2	1100p
	Malachite	CO_3^{2-}	1400p, 1500p
	Gypsum	$CaSO_4{\cdot}2H_2O$	1640p
	Malachite	HO^-	3350p, 3450p
MA4	Sulphide/tin oxide	SnO_3^{2-}	300p
	Zincit/quarz	$ZnCO_3/SiO_2/SnO$	480m
	Tenorite/aluminate	CuO/AlO_2^-	510p, 590m, 750p, 820p
	Malachite/calcite	CO_3^{2-}	880p
	Atacamite/paratacamite	SO_4^{2-}	1050p
	Quarz	SiO_2	1100m
	Malachite	CO_3^{2-}	1400p, 1500p, 1650m
	Malachite	HO^-	3350p, 3450p
MA5	Tin oxide	SnO_3^{2-}	305p
	Zincite/quarz	$ZnCO_3/SiO_2/SnO$	480p
	Tenorite	CuO	520p, 600m, 820m
	Malachite/calcite	CO_3^{2-}	900m
	Atacamite/paratacamite	SO_4^{2-}	1050f
	Malachite/azurite/calcite	CO_3^{2-}	1400p, 1500m, 1650s
	Malachite/azurite	HO^-	3350p, 3450p
MA6	Tin oxide	SnO_3^{2-}	300p
	Zincite/quarz	$ZnCO_3/SiO_2/SnO$	480m
	Tenorite	CuO	520m, 600m, 820m
	Malachite/calcite	CO_3^{2-}	900m, 980p
	Atacamite/paratacamite	SO_4^{2-}	1050p
	Quarz	SiO_2	1100m
	Malachite/azurite/calcite	CO_3^{2-}	1400p, 1500m, 1650m
	Malachite/azurite	HO^-	3350p, 3450p

Table 5 Chemical compounds determined by XRD in corrosion products and contaminants

Mineral phase	Chemical formula	Color and aspect	No pick	PDF	MA 1	MA2	MA3	MA4	MA5	MA6
Malachite	$CuCO_3{\cdot}Cu(OH)_2$ or $Cu_2(OH)_2CO_3$	Green, with a characteristic vitreous aspect	22	10–399	+++	+++	++	++	+	+
Azurite	$2CuCO_3{\cdot}Cu(OH)_2$ or $Cu_3(OH)_2(CO_3)_2$	Dark blue	20	11–136 11–682	++	++	++	++	–	–
Atacamite	$Cu_2(OH)_3Cl{\cdot}nH_2O$ or $CuCl_2{\cdot}3Cu(OH)_2{\cdot}nH_2O$	Emerald green with more or less dark tones in function of *n* and with a vitreous aspect	62	2–0146 25–0269	++	++	+	+	–	–
Parathacamite	$Cu_2(OH)_3Cl$ $CuCl_2{\cdot}3Cu(OH)_2$	Green blue	20	15–694 19–389 25–1427	++	++	+	+	–	–
Nantokite	Cu_2Cl_2	Waxy grey white	1	6–0344	+	+	+	+	+	+
Cuprite	Cu_2O	Brick red, with grey brownish or yellowish to orange tones	76	5–0667	++	++	++	++	++	++
Tenorite	CuO	Black grey to brown	1	41–0254	+	+	+	+	+	+
Cassiterite	SnO_2	Shiny white	2	6–0395	+	+	–	–	–	–
Minium	Pb_3O_4	Red	1	29–0781	+	+	+	+	–	–
Calcocite	Cu_2S	Pb-like grey, with metallic brightness	2	9–0328 33–0490	+	+	++	++	++	++
Calconite	$CuSO_4{\cdot}5H_2O$	Clear blue	33	21–0816 36–0432	++	++	+	+	+	+
Antlerite	$Cu_3(OH)_4SO_4$ or $CuSO_4{\cdot}2Cu(OH)_2$	Blackish with green tones	16	7–0407	++	++	+	+	–	–
Brochantite	$Cu_4(OH)_6SO_4$ or $CuSO_4{\cdot}3Cu(OH)_2$	Blue to clear green	83	13–0398 43–1458	++	++	+	+	+	+
Langite	$Cu_4(OH)_6SO_4{\cdot}H_2O$ or $CuSO_4{\cdot}3Cu(OH)_2{\cdot}H_2O$	Dark bright green	4	20–0364	++	++	++	++	++	++
Anglesite	$PbSO_4$	Grey – greenish grey	20	5–0577 36–1461	+	+	+	+	–	–
Cerrusite	$Pb_2(OH)_2CO_3$	White	2	13–0131	+	+	+	+	–	–
Gloslarite	$ZnSO_4{\cdot}7H_2O$	Grey with opalescent reflexes	5	36–1451	+	+	+	+	+	+
Gypsum	$CaSO_4{\cdot}2H_2O$	White grey	33	21–0816 36–0432	+	+	–	–	–	–
Quarz	SiO_2	Translucent grey	7	5–0490	+	+	–	–	–	–
Calcite	$CaCO_3$	White grey	14	5–0586 24–0027	++	++	–	–	–	–
Organic substances		Black brownish	2	28–2016 31–1982	+	+	–	–	–	–

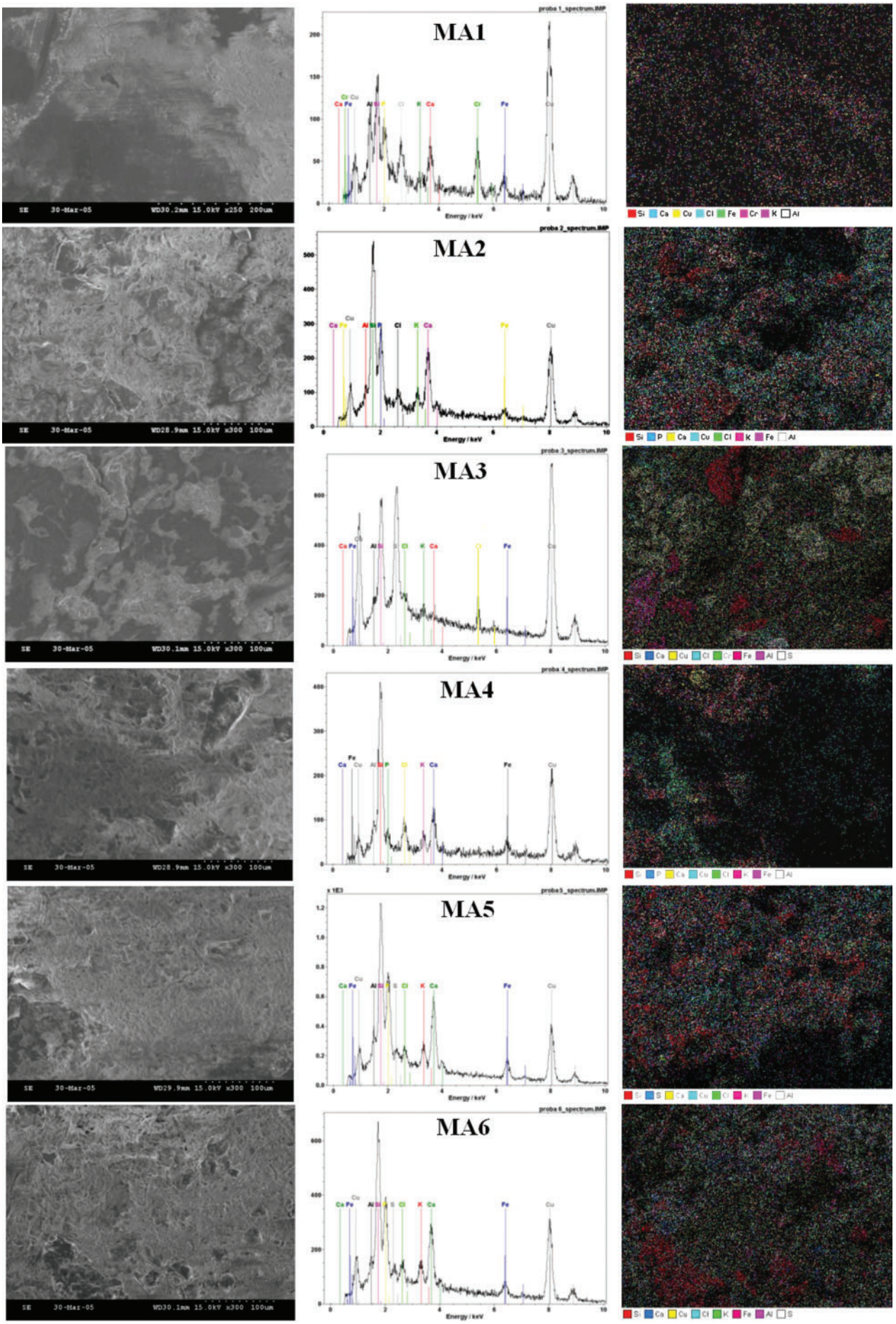

4 Scanning electron microscopy coupled with EDX for six coins

site (non-disturbed or disturbed), the archaeological patina can have compositions and mineralogical distributions with specific dispersions, i.e. stratified or not. The detailed study of the structural characteristics of the archaeological patina allows the identification of the structural–phenomenological correlations.

The present study analyses six coins from the eleventh and twelfth centuries B.C., discovered in 2000 in the Nufărul site (Tulcea County, Romania), initially classified for the 'grey fund' because of their precarious conservation state (thin and fragile metallic bulk or very thin, discontinuous and even absent one). These coins have been discovered separately over a 600 m^2 at the site together with some well preserved gold and silver coins (from the period of Constantine VII to Roman II, 945–959 A.D.), which have been classified for museum display. The main questions about them refer to their being made from the same mineral and to their emission period and circulation area. By using a system of five modern techniques, namely the optical microscopy, colorimetric reflection, IR spectroscopy, XRD and SEM-EDX, the following aspects have been rendered evident.

1. The coins are from different manufactured lots or locations, because they have three basic alloy compositions. However, although they have the same age, the conservation state of the metallic bulk is different. This aspect is a result of the different material resistance because of the original composition and manufacture.

2. The correlation of the data resulting from the microchemical analyses coupled with the mineralogical and colorimetric ones as well as with those obtained from the IR spectroscopy and the SEM-EDX has allowed the establishment of the similitude between the coins with three basic alloys. These are Byzantine coins of Dobrogea, containing in their composition Cu, Sn, Zn, Pb, Cr and Fe for the MA1 and MA3, Cu, Sn, Zn, Pb, for the MA2 and MA4, Cu, Sn, Zn, Fe for the MA5 and MA6 respectively;

3. Because the Pb, Cr and Fe cations, as alloy microelements, are not present in all the coins, this fact demonstrates that the coins were originally made at different locations, sources or from different ores.

4. Furthermore, analytical SEM coupled with the EDX has proved successful in differentiating the chemical products of the primary and secondary patinas, versus those from contamination using dispersion mapping of the elements over the surface.

References

1. I. Sandu, A. Dima and I. G. Sandu: 'Conservation and restoration of metallic artifacts'; 2002, Iasi, Corson.
2. I. Sandu, C. Marutoiu, I. G. Sandu, A. Alexandru and A. V. Sandu: *Acta Univ. Cibiensis – Chem.*, 2006, **9**, 39–53.
3. I. G. Sandu, S. Stoleriu, I. Sandu, M. Brebu and A. V. Sandu: *Rev. Chim.*, 2005, **56**, 981–994.
4. W. Mourey: 'Conservation of metallic antiquities – from archaeological site to museum'; 1998, Bucharest, Tehnica.
5. I. G. Sandu, I. Sandu and A. Dima: in 'Modern aspects concerning the conservation of works of art – Vol. III: Authentication and restoration of artifacts from inorganic materials'; 2006, Iasi, Performantica.
6. R. Mazzeo: 'Kermesquaderni', 29–43; 2005, Firenze, Nardini.
7. G. M. Ingo, E. Angelini, T. de Caro, G. Bultrini and I. Calliari: *Appl. Phys. A*, 2004, **79A**, 199–205.
8. I. Montero, G. Demortier, J. L. Ruvalcaba-Sil, A. Climent-Font, C. Palacio and D. Diaz: *Nucl. Instr. Meth. Phys. Res. B*, 1998, **234B**, 229–238.
9. C. V. Horie and J. A. Vint: *Stud. Conserv.*, 1982, **27**, 185.
10. J. D. Meakin, L. D. Ames and D. A. Dolske: *Atm. Environ. B*, 1992, **26B**, 207.
11. D. A. Scott: 'Copper and bronze in art: corrosion, colorants, conservation'; 2002, Los Angeles, CA, The Getty Conservation Institute.
12. I. Constantinides, A. Adriaens and F. Adams: *Appl. Surf. Sci.*, 2002, **189**, 90–102.
13. O. Damian, C. Andone and M. Vasile: *Cronica Cercetarilor Arheologice din Romania*, 2001, **5**, 164–165.
14. L. S. Selwyn, N. E. Binnie, J. Poitras, M. E. Laver and D. A. Downham: *Stud. Conserv.*, 1996, **41**, 205.
15. I. Sandu, I. C. A. Sandu and I. G. Sandu: 'Colorimetry in art'; 2002, Iasi, Corson.
16. K. Nassau, P. K. Gallancher, A. E. Miller and T. E. Graedel: *Corros. Sci.*, 1987, **27**, 669.
17. ICDD: 'JCPDS mineral file: joint committee for powder diffraction inorganic search manual', Swarthmore, International Centre for Diffraction Data, 1992.
18. F. F. Bentley, L. D. Smithson and A. L. Rozek: 'Infrared spectra and characteristic frequences: A collection of spectra, interpretation and bibliography'; 1515–1566; 1988, New York, London, Sydney, John Wiley & Sons.